

Article

Removal of Nano-Zinc Oxide (nZnO) from Simulated Waters by C/F/S—Focusing on the Role of Synthetic Coating, Organic Ligand, and Solution Chemistry

Rizwan Khan ^{1,*} , Muhammad Ali Inam ² , Ick Tae Yeom ³, Kang Hoon Lee ⁴  and Kashif Hussain Mangi ¹ 

¹ Department of Chemical Engineering, Quaid-e-Awam University of Engineering, Science and Technology (QUEST), Nawabshah 67480, Pakistan; kashifmangi@quest.edu.pk

² School of Civil and Environmental Engineering (SCEE), Institute of Environmental Sciences and Engineering (IESE), National University of Sciences and Technology (NUST), H-12 Campus, Islamabad 44000, Pakistan; ainam@iese.nust.edu.pk

³ Graduate School of Water Resources, Sungkyunkwan University (SKKU), Suwon 16419, Republic of Korea; yeom@skku.edu

⁴ Department of Energy and Environmental Engineering, The Catholic University of Korea, 43 Jibong-ro, Bucheon-si 14662, Republic of Korea; diasoyong@catholic.ac.kr

* Correspondence: rizwansoomro@quest.edu.pk

Abstract: Increased usage of nano-zinc oxide (nZnO) in different commercial fields has raised serious concerns regarding their discharge into the water streams containing natural and synthetic coating agents. Moreover, utilization of ground and surface water for drinking purposes is a common approach in many countries. Therefore, the removal of nZnO particles from water is essential to minimize the risk to the environment. The present research investigated the removal of nZnO from complex water matrices by conventional coagulation-flocculation-sedimentation (C/F/S) process using polyaluminum chloride (PACl) as coagulants. The result showed that removal of uncoated nZnO through sedimentation was efficient in waters containing divalent cations in the absence of dissolved organic matter (DOM). For the water containing higher salt concentration, PACl coagulant showed better removal performance with increasing coagulant dosage; however, synthetic organic coating agent and DOM significantly decreased the removal up to 75%. The surface potential of studied waters indicated that the addition of PACl affects the charge potential of nZnO particles resulting in charge neutralization. The result of the particle size analyzer revealed the presence of smaller particles with size of 430 nm even after C/F/S process, which may increase the possibility of particles release into aquatic environment. The results of the present study may help in understating the removal behavior of other coated nanoparticles during conventional water treatment.

Keywords: synthetic coating; water; zinc oxide; coagulation



Citation: Khan, R.; Inam, M.A.; Yeom, I.T.; Lee, K.H.; Mangi, K.H. Removal of Nano-Zinc Oxide (nZnO) from Simulated Waters by C/F/S—Focusing on the Role of Synthetic Coating, Organic Ligand, and Solution Chemistry. *Processes* **2023**, *11*, 2604. <https://doi.org/10.3390/pr11092604>

Academic Editors: George Z. Kyzas, Choon Aun Ng, Mohammed J. K. Bashir and Ping Zeng

Received: 9 August 2023

Revised: 26 August 2023

Accepted: 29 August 2023

Published: 31 August 2023



Copyright: © 2023 by the authors. Licensee MDPI, Basel, Switzerland. This article is an open access article distributed under the terms and conditions of the Creative Commons Attribution (CC BY) license (<https://creativecommons.org/licenses/by/4.0/>).

1. Introduction

Climate change affected the water resource and increased water scarcity; therefore, it is a common strategy to effectively utilize the available aquatic sources such as ground and surface water for public as well as commercial purposes. Moreover, engineered nanoparticles (ENPs) have been a focus of research interest due to their unique physicochemical properties. Among many nanomaterials, nano-zinc oxide (nZnO) is widely used in different products and commercial applications, due to its novel mechanical and catalytic properties [1]. The worldwide yearly production of nZnO was expected to be 1600–58,000 tons/year with market growth of USD 400 million by 2020 [2,3]. The increased production and incorporation of nZnO in many consumer items raises serious concern that they may eventually be released into the water streams leading to potential damage to environment. Moreover, 50% of annually produced ENPs are predicted to be released into the water streams directly (consumer products) or indirectly. A few researchers have simulated the

probable concentration of ENPs in the environment [4,5]. The effluent from water treatment plants (WTP) is assessed to be 1200–29,200 tons annually into water bodies globally [6]. Thus, WTP provides a substantial pathway for ENPs, specifically nZnO.

Nanomaterials such as nZnO pose substantial health as well as environmental risk to the ecosystem. These tiny particles may enter the human body directly (ingestion) or indirectly (bioaccumulation) [7]. Earlier studies [8,9] have reported toxicity of nZnO to various biota, i.e., mammalian, earthworms, plants, and sea urchin. Most of the released nZnO have active materials with organic coating for longer stabilization, thereby enhancing the relative toxicity. Consequently, it is significant to understand the removal of nZnO by conventional WTP to eliminate its adverse effect on the aquatic environment and human health due to its exposure.

Recently, the effect of ENPs size, concentration, and type on the coagulant dosage and total performance of the system was well demonstrated by Popowich et al. [10]. Moreover, the process conditions, i.e., solution pH and electrolyte concentration, play an essential role in enhancing the efficiency of treatment process. Rozman et al. demonstrated the enhanced mobility of TiO₂ and nZnO in the aquatic environment due to the adsorption onto microplastic surface [11]. Consequently, it is significant to explore the removal of ENPs from complex water environments, using the chemical coagulation process. Several studies [12,13] have reported that the occurrence of dissolved organic matter (DOM) affects the colloidal behavior of ENPs in aquatic system. The lower concentration of DOM in the water containing monovalent ions increases the stability of ENPs agglomerates such as copper oxide (CuO) nanoparticles, thereby reducing the risk to water environment [14]. In contrast, it has been also demonstrated that higher DOM concentration reduces the size of NPs aggregates and stabilizes the colloids by electrostatic hindrance [15]. The other influential parameters for colloidal stability, agglomeration, and toxicity are the synthetic organic coatings used in many industrial applications as well as commercial products. In industrial applications, the agglomeration of NPs is controlled by organic coatings such as meso-2,3-dimercaptosuccinic acid (DMSA), which has been utilized in different medical and environmental applications [16]. Moreover, this coating (DMSA) simultaneously acts as chelating agent that is able to bind metal ions to form a complex ring structure called chelates, which possess ligand binding atoms that can form one or two covalent bonds [17]. Many researchers reported that the presence of DMSA coating forms strong complexes with the surface layer of the iron-oxide (maghemite) NPs and enhanced stability in intracellular uptake due to unbound carboxylate groups [18,19]. DMSA has been also utilized as capping agent for quantum dots and maghemite NPs. Therefore, it is important to explore the fate, mobility, and agglomeration behavior of nZnO in the presence of synthetic coatings.

Mostly, treatment methods, i.e., chemical coagulation, flocculation, and filtration followed by chemical oxidation are introduced by the WTP after secondary treatment unit to further clean the effluent before discharge. Many researchers have investigated the removal of ENPs from water and wastewater by activated sludge, reverse osmosis, electro-coagulation, and coagulation-flocculation-sedimentation (C/F/S) process. A recent study reported above 80% removal of CeO₂ NPs from drinking water using granular activated carbon [20]. Previous studies have shown that traditional C/F/S technology is effective in the removal of suspended colloids, DOM, inorganic matter, microplastic and disinfection by-product from contaminated water [21,22]. A recent study [6] demonstrated that metal salts (i.e., aluminum, iron) are efficient in removal of suspended colloids and DOM; however, removal performance is significantly affected by solution chemistry and type of organic ligands. The presence of DOM such as fulvic and humic acid can adsorb onto the nZnO surface, thus altering their structural as well as physio-chemical properties. A recent study [23] reported the better removal of titanium dioxide (TiO₂) using aluminum coagulant in waters containing high molecular weight hydrophobic organic ligands. Moreover, if the DMSA nanometals are discharged into the freshwater which contains the various salts and DOM, this may further enhance their mobility and transformation behavior. Even with the exposure and concentration assessment of nanoparticles, we are still faced with

a lack of quantitative knowledge and appropriate methods for detecting, characterizing, and quantifying NPs in complex natural media. Many researchers have only focused on the potential toxicity of NPs along with their treatment pathways in simple environment; however, limited literature has focused on the removal of NPs in complex water environment using a conventional process such as C/F/S. If WTP fails to remove these toxic contaminants, they may enter the human body through ingestion of water. Thus, it is essential to investigate the ability of conventional techniques to remove nZnO in the presence of DOM and synthetic coatings.

As a result, the present research aimed to investigate the ability of C/F/S process to remove nZnO NPs. The specific objectives were to explore the influence of monovalent salt (NaCl), synthetic source water (i.e., surface and ground waters), organic coating (DMSA), and presence of DOM on the removal of nZnO.

2. Materials and Methods

2.1. Chemicals and Reagents

Uncoated (bare) nanopowder of zinc oxide (CAS No: 1314-13-2, purity > 97%), humic acid (HA), and meso-2,3-dimercaptosuccinic acid (DMSA) were procured from Sigma Aldrich (St. Louis, MO, USA). The coated nZnO was prepared by the earlier described method [24] using DMSA as the coating agent. Polyaluminum chloride (PACl) with (65–70% basicity) in stock solution with (850 mg/L Al₂O₃) was obtained from Elf Atochem (Toulouse, France) and used in C/F/S experiments.

2.2. Preparation of Test Solution

The stock solution of obtained nanopowder of zinc oxide was prepared by adding nZnO powder into deionized water. Firstly, 1000 mg/L of nZnO stock suspension was prepared and pH of the suspension was adjusted to 7.0 using 0.1 M HCl or NaOH. The nano-ZnO suspension was sonicated using Bio-safer ultrasonicator (Nanjing, China) for 40 min at 500 W to obtain stable NPs suspension. The stock suspension of nZnO was diluted into a desired concentration and used in the C/F/S experiments. The present research was carried out using different media conditions including synthetic surface water (SSW), synthetic ground water (SGW), and two different concentrations of ionic strength (IS) of NaCl. The monovalent salt IS content of 2.5 and 10 mM was chosen to compare with electrolyte content of SSW [25] and SGW [26], respectively. The pH of solution used in the present study was controlled at 7.5 by 100 mM NaOH or HCl to simulate the pH of natural SSW and SGW. A detailed list of constituents for SSW and SGW is presented in Table 1. HA was used to represent the model organic ligand, about 1 mg/L of concentration was selected to depict the natural surface and ground waters [27,28].

Table 1. Composition of synthetic waters.

Synthetic Surface Water (SSW)	Concentration (mg/L)	Synthetic Ground Water (SGW)	Concentration (mg/L)
MgCl ₂ 6H ₂ O	16.5	CaCl ₂ 2H ₂ O	107.1
MgSO ₄	8.30	CaSO ₄ 2H ₂ O	74.4
KHCO ₃	3.10	KNO ₃	59.5
NaHCO ₃	19.3	NaHCO ₃	107.1
CaCO ₃	33.0	Ca(NO ₃) ₂ 4H ₂ O	104.2
-	-	MgSO ₄ 7H ₂ O	178.6
Total	80.2		630.9

2.3. C/F/S Experiments

The C/F/S experiments were performed at room temperature using an automatic jar tester with six mixing paddles. For all the experiments, a jar with capacity of 2 L was used. In all experiments, a predetermined dosage of PACl (50 mg/L) was used to enhance the sweep flocculation process, which is typically used in WTP. Moreover, the initial concentration of bare and coated nZnO was fixed at 100 mg/L in C/F/S experiments. Prior to each experiment, the nZnO suspension was probe sonicated for 2 min to separate the large agglomerates. The solution was rapidly mixed for 1 min at 150 rpm to ensure a velocity gradient equal to or greater than 1000 s^{-1} . Thereafter, the flocculation suspension was slowly mixed at 30 rpm for 30 min to keep the speed gradient of around 30 s^{-1} . The parameter such as flocculation velocity gradient was based on typical reactor designs used in drinking WTP. In the final step, the sedimentation was carried out at 0 rpm and suspension was left for 60 min to allow the colloids to settle down. After completion of the experiment, the aliquots were collected below 2 cm for the analysis of nZnO concentration, ζ -potential, and hydrodynamic diameter (HDD). The concentration of nZnO NPs in collected sample was measured using an Optizen UV-Vis spectrophotometer at wavelength of 370 nm as reported in earlier studies [29]. A control experiment was also performed without any coagulant (0 mg/L) to determine the efficacy of the coagulant and interaction of nZnO with PACl coagulant. The ζ -potential was analyzed through (Nano ZS90, Worcestershire, UK). All experiments were performed in triplicates and relative standard deviations were plotted in the graphs.

2.4. Analytical Measurement

The ζ -potential (mV) was determined at room temperature with 10 repeated measurements, where the refractive indices of nZnO and water were set to 2.00 and 1.33, respectively. The Fourier transform infrared (FTIR) (JASCO Analytical Instruments, Easton, PA, USA) analyses of pristine nZnO, DMSA, and DMSA-coated nZnO were performed. X-ray diffractometry (XRD) of pristine nZnO and DMSA-coated nZnO were analyzed using Dmax C III (Rigaku Corporation, Tokyo, Japan). The residual concentration of nZnO particles ($>0.45\text{ }\mu\text{m}$) was analyzed through inductively coupled plasma coupled with mass spectrometry (ICP-MS).

3. Results

3.1. Characterization of Uncoated and Coated nZnO NPs

The FTIR spectra of pristine DSMA, nZnO, and DSAM-coated nZnO particles are shown in Figure 1A. The absorption band at 3375 cm^{-1} was attributed to O-H vibrations due to moisture content in sample. The peaks at 2563 cm^{-1} and 1715 cm^{-1} in DMSA sample was attributed to the S-H and C=O stretching of the carboxylic groups, respectively [30]. These spectrum bands were visible in the DMSA-coated nZnO with slight shifts confirming the coating of DMSA onto the nZnO NPs surface. The XRD pattern of uncoated nZnO and DMSA-coated nZnO was measured to analyze any changes in crystalline structure. Even though DMSA was coated onto nZnO surface, insignificant difference in the nZnO crystalline structure between the uncoated nZnO and DMSA-coated nZnO was observed [31]. This confirms that the surface coating of DMSA did not affect the crystalline structure of the ZnO core particles, which means the nZnO NPs were stable even after surface modification.

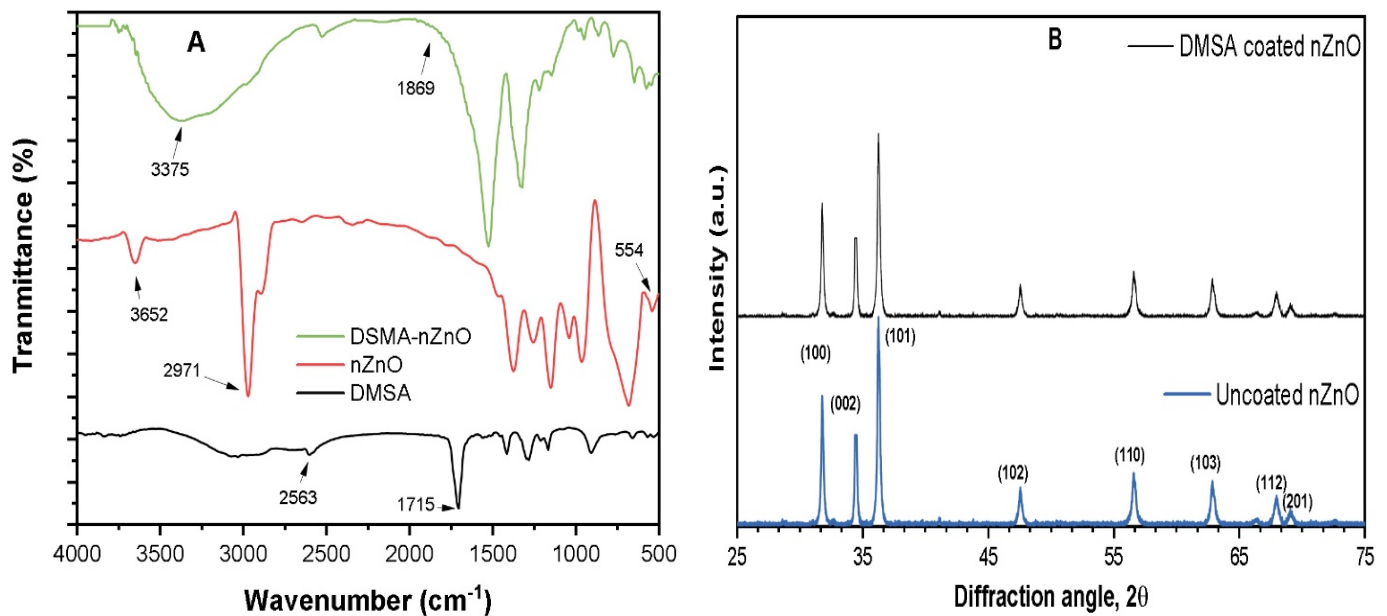


Figure 1. (A) FTIR spectra of pristine DMSA, nZnO, and DMSA-nZnO coated particles; (B) XRD of pristine nZnO and DMSA-nZnO coated.

3.2. Influence of IS and Solution Chemistry on the Removal of nZnO Particles

Figure 2A showed better removal of uncoated nZnO in complex environmental water SGW (98%) and SSW (99%), respectively than with the monovalent salt containing waters of 2.5 mM NaCl (74%) and 10 mM NaCl (83%), respectively. The formation of hydrolyzed species ($\text{Al}(\text{OH})_4^-$) in the solution resulted in effective particle destabilization [32]. Further increase in PACl dosage may enhance the cationic species in the system, thus leading to the charge reversal and destabilization of colloids [33]. The observed (Figure 2B) positive ζ -potential of nZnO system is due to the excess absorption of the positively charged Al species. Moreover, the excessive PACl dosage (50 mg/L) above the optimum point may lead to precipitation of amorphous hydroxide (OH) colloids [33]. The combined effect of positively charged OH and cationic species results in excess surface charge of the nZnO NPs as observed in Figure 2B.

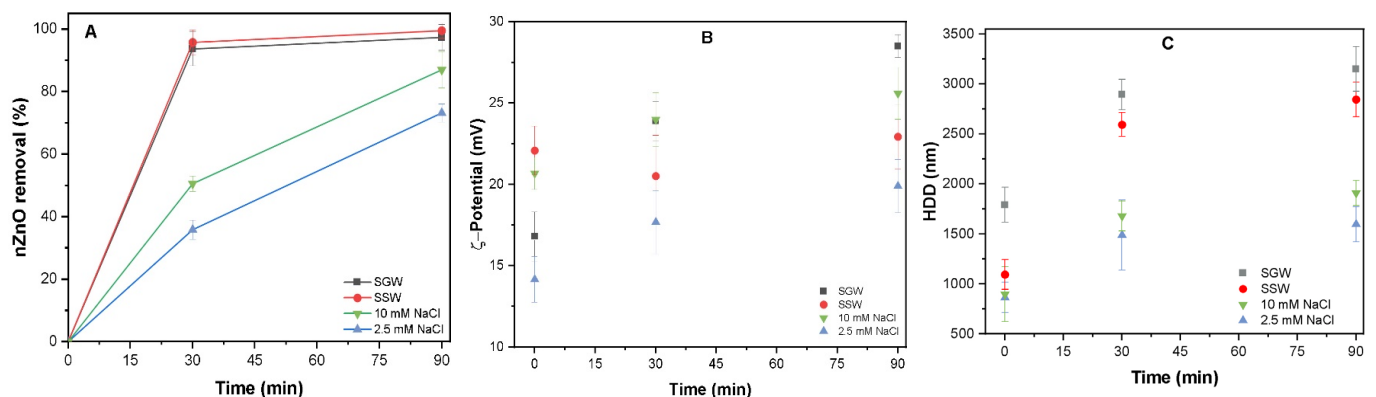


Figure 2. (A) Removal of uncoated nZnO (100 mg/L) in all four studied waters of 2.5 mM NaCl, 10 mM NaCl, 2.5 mM SSW, and 10 mM SGW at PACl (50 mg/L); (B) ζ -potential (mV) and (C) HDD of nZnO in all four waters.

The removal performance with increasing electrolyte concentration within each respective system (NaCl vs. synthetic waters) shows insignificant change ($p > 0.05$). The nZnO dispersed in the NaCl system shows enhanced stability with surface potential of 19.6 and 25.1 mV for 2.5 and 10 mM NaCl, respectively, as compared to synthetic waters with potential of 14.1 and 19.2 mV for SGW and SSW. Our results agree with the observation in previously reported NaCl-containing waters [34]. Moreover, the measured particle size in the different studied waters of 2.5 mM NaCl, 10 mM NaCl, SGW, and SSW were 1523.0, 1759.0, 2732, and 3221 nm, respectively as shown in Figure 2C. The reduction in the colloidal stability may be correlated with the enhanced removal performance in SSW and SGW at flocculation as well as sedimentation stages of treatment. The enhanced removal efficiency in the synthetic natural waters (SGW and SSW) may be due to the presence of divalent cation (i.e., Mg^{2+} , Ca^{2+}), thereby reducing the colloidal stability. The divalent cations such as Ca^{2+} and Mg^{2+} due to their larger outer valance size efficiently compressed the electrical double layer (EDL) near the colloid surface than monovalent ions (i.e., NaCl, KCl). This may also be attributed to the effective charge screening and reduced Debye length [29]. The increased removal of (above 98%) was observed in waters (SGW and SSW) containing the divalent cations. Previous study reported similar results, wherein the presence of Ca^{2+} ions result in increased NPs agglomeration [35]. The improved removal may also be due to the presence of highly charged anions, which increase the OH precipitation enmeshing the nZnO NPs to form larger size flocs that easily settle down.

3.3. Role of DOM in Removal of Uncoated nZnO

In WTP, the occurrence of organic ligand may affect the removal and mobility of NPs; thus, the effect of DOM was investigated in all studied waters. Figure 3A shows that the presence of DOM in the system significantly affected the removal of uncoated nZnO NPs as compared to those without DOM. The removal efficiencies in different systems of 2.5 mM NaCl, 10 mM NaCl, SGW, and SSW, were observed to be 19.8%, 51.0%, 71.1%, and 73.0%, respectively. The DOM contains various phenolic and carboxylic functional groups that might adsorb onto the nZnO surface, which results in the repulsion amongst the charged precipitates. The enhanced removal of nZnO in systems containing the higher electrolyte content was observed, which might be due to the charge neutralization in the suspension.

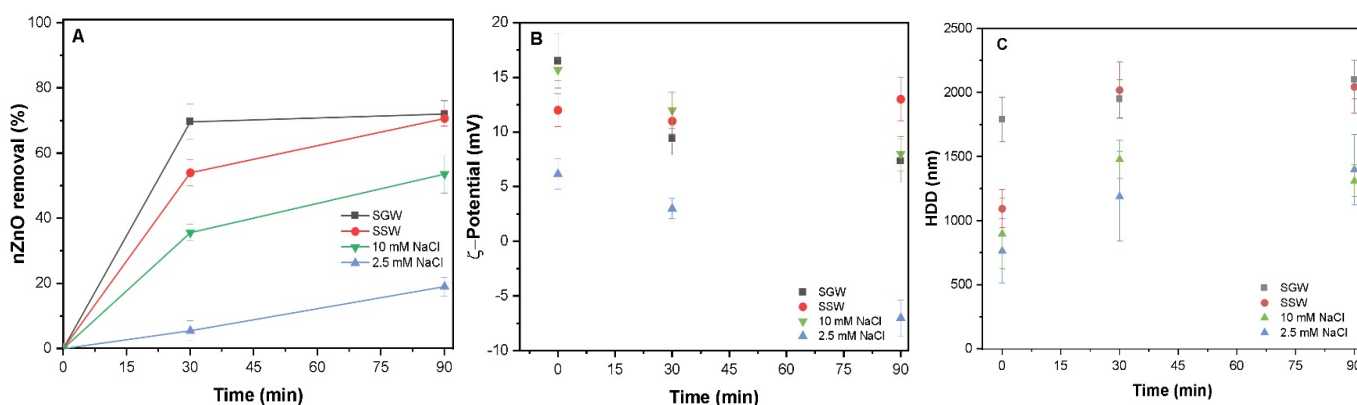


Figure 3. (A) Removal of uncoated nZnO (100 mg/L) and DOM in all four studied waters of 2.5 mM NaCl, 10 mM NaCl, 2.5 mM SSW, and 10 mM SGW at PACl (50 mg/L); (B) ζ -potential (mV) and (C) HDD of nZnO in all four waters.

The measured ζ -potential in these waters of 2.5 mM NaCl, 10 mM NaCl, SGW, and SSW were -4.1 , 12.0 , 13.1 , and 7.3 mV, respectively. These observations are in good agreement with the low removal in water containing less amount of salt content (Figure 3A). This may be attributed to the interaction between the positively charged OH species and negatively charged functional groups of DOM [12]. However, the removal trends in simulated SSW and SGW were almost similar, indicating that the dominant sweep flocculation mechanism,

resulting in enhanced OH precipitation, is associated with the highly charged anions. The reduction in the size of aggregates was observed in the presence of DOM (Figure 3C), then without DOM (Figure 2C), which might be due to the steric repulsion of sorbed DOM on the surface of nZnO. The measured HDD of nZnO in different waters of 2.5 mM NaCl, 10 mM NaCl, SGW, and SSW were 1354, 1490.2, 2106, and 2016 nm, respectively. The size of aggregates enhanced substantially ($p < 0.05$) with increasing the electrolyte concentration within the NaCl-containing waters after sedimentation. Moreover, the size of agglomerates between the NaCl and synthetic waters notably increased ($p < 0.05$); however, this difference was insignificant ($p > 0.05$) in SSW and SGW. This might be ascribed to the fact that with enhancing IS of monovalent ions, the electrostatic repulsion is screened, and the energy barrier shrinks [36]. The larger agglomerates after flash mixing were observed at 2.5 mM NaCl as compared to 10 mM NaCl, which might be due to the weak interaction amongst the DOM and nZnO NPs surface results in the enhanced polymer bridging between colloids to form large aggregates (Figure 3C). In contrast, the stronger interactions between the DOM and precipitate surface might enhance the particle stability due to electrostatic repulsion [13]. Previous studies [11,18] reported the increased stability of NPs in monovalent and divalent cations at different solution chemistries owing to electrostatic hindrance. In simulated waters, the presence of divalent ions effectively compresses the EDL around the particle than monovalent ions such as NaCl systems [23]. Moreover, neutralization of surface charge of nZnO induced counter ions owing to destabilization and subsequent agglomeration. Elimelech et al. reported similar observations during the kinetic study of fullerene (C60) NPs in the presence of divalent cation and HA-coated surface, where macromolecules rapidly form complexes with cations, thereby reducing the steric hindrance effect of sorbed macromolecular layers [37].

3.4. Role of DMSA Coating and DOM on Removal of nZnO

The synthetic coating has been widely used to stabilize commercial nanoparticles in different products and applications that might be released into water treatment facilities. In the present study, the effect of the simultaneous presence of DOM and synthetic coating (DMSA) has been investigated under environmentally relevant conditions. The removal efficiencies of DMSA-coated nZnO NPs at different waters of 2.5 mM NaCl, 10 mM NaCl, SGW, and SSW systems were observed to be 51.0%, 77.8%, 63.6%, and 99.1%, respectively (Figure 4A). In NaCl system, the total removal after sedimentation was found to be statistically insignificant, demonstrating that monovalent electrolytes had little effect, similar to the previous results of uncoated nZnO NPs. The measured ζ -potential of 2.5 mM NaCl and 10 mM NaCl were 16.5 and 20.1 mV, respectively (Figure 4B). In general, the presence of synthetic organic coating caused a slight decrease in removal, which might be due to the steric repulsion of ligand coating onto nZnO. These observations are in good agreement with the results of DLS showing smaller size aggregates in these waters (Figure 4C). The presence of carboxylic groups in DOM might contribute to more negative charges on the nZnO surface after ionization at pH 7, thereby causing significant decline in van der Waals forces [11]. An increase in SGW removal was observed as compared to NaCl-containing waters and SSW system. The enhanced screening in the presence of different divalent cations reduces the surface potential (Figure 4B) and rapid precipitation due to the fact that strongly charged anions increase the size of agglomerates (Figure 4C). Moreover, the improved removal in the 10 mM NaCl system might be ascribed to the chelation of the DMSA between the nZnO and hydroxide precipitates, decreasing the stability of NPs offered by DOM. Thus, minimal impact of synthetic organic coating was observed on the fate and mobility of nZnO NPs as compared to without synthetic coating in the presence of DOM within the water treatment process.

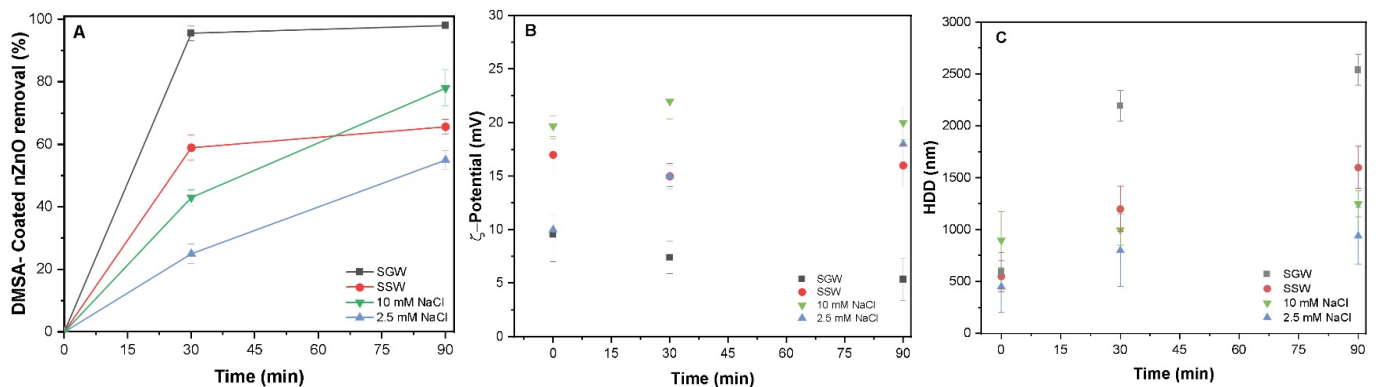


Figure 4. (A) Removal of DMSA-coated nZnO (100 mg/L) in all four studied waters of 2.5 mM NaCl, 10 mM NaCl, 2.5 mM SSW, and 10 mM SGW at PACI (50 mg/L); (B) ζ -potential (mV) and (C) HDD of nZnO in all four waters.

The removal of DMSA-coated nZnO and DOM in waters of 2.5 mM NaCl, 10 mM NaCl, SGW, and SSW was found to be 80.1%, 78.9%, 61.3%, and 59.2%, respectively, Figure 5A. The surface potential in studied waters of 2.5 mM NaCl, 10 mM NaCl, SGW, and SSW was measured to be 8.5, 6.3, 13.2, and -5.5 mV, respectively, Figure 4B. Remarkably, the removal behavior in NaCl of only system and natural synthetic waters (SGW and SSW) showed an inverted trend, similar to the obtained removal behavior of nZnO NPs in the presence of DOM. The synthetic coating might enhance the interaction between DOM surface, thereby reducing the attachment of chain segment into the suspension, and then promoting agglomeration [25]. Subsequently, the lower removal of DMSA-coated nZnO NPs in synthetic waters than in waters containing only DOM might be due to the chelation of DMSA and metal ions, i.e., Ca^{2+} or Mg^{2+} , thereby reducing the available active site for bridging [29]. These results are supported by the substantially larger size aggregates observed in SGW (Figure 5C), which contains more Ca^{2+} content than the other three waters.

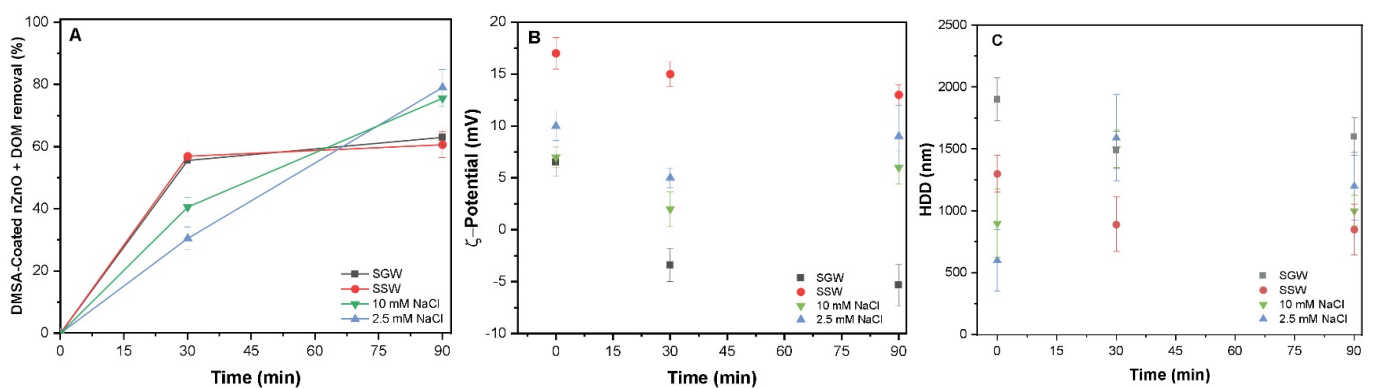


Figure 5. (A) Removal of DMSA-coated nZnO (100 mg/L) + DOM in all four studied waters of 2.5 mM NaCl, 10 mM NaCl, 2.5 mM SSW, and 10 mM SGW at PACI (50 mg/L); (B) ζ -potential (mV) and (C) HDD of nZnO in all four waters.

It was observed that even under higher removal conditions above 95%, smaller amount of NPs aggregates remain suspended in the solution. Thus, the concentration of nZnO aggregates colloids smaller than 0.45 μm was measured using 5 ppm solution (Table 2). The results indicated that despite aggregation-inducing compounds and coagulants, there is still a major concern about the released colloids in small aggregates via conventional WTP. Thus, the release of these particles increases the risk to human health and environment due to their enhanced reactivity, mobility, and transport in the ecosystem.

Table 2. ICP-MS data collected for jar tests after sedimentation.

Experimental conditions	ICP Concentration (ppm)			
	2.5 mM NaCl	10 mM NaCl	SSW	SGW
Uncoated nZnO	4.55–0.01	4.54–0.02	4.62–0.02	4.56–0.02
Uncoated nZnO + DOM	4.63–0.01	4.79–0.01	4.59–0.01	4.63–0.02
DMSA-coated nZnO	4.60–0.02	4.62–0.01	4.64–0.02	4.60–0.03
DMSA-coated nZnO + DOM	4.65–0.00	4.61–0.02	4.75–0.11	4.73–0.07

4. Conclusions

The objective of the present research study was to investigate the impact of synthetic organic coating, DOM, and water chemistry on nZnO NPs removal by C/F/S process. The findings showed that the removal of uncoated nZnO NPs through settling was efficient (>90%) in high electrolyte concentration and specifically divalent cations without DOM. The removal efficiency of DMS-coated nZnO NPs in the presence of DOM decreased up to 75%, with reduction in the size of aggregates owing to the steric repulsion effect of sorbed DOM compounds. The C/F/S experiments showed that high dosages of polyaluminum-based coagulants can efficiently remove the nZnO NPs; however, under complex environmentally relevant conditions, the smaller NPs with size of 430 nm remain suspended after sedimentation. Findings showed that the main mechanism involved in the removal of DMSA-coated nZnO NPs might be swept flocculation and charge neutralization. The study provides some insight into the influence of synthetic organic coating and DOM on the fate, mobility, and removal of released nZnO during the water treatment process.

Author Contributions: Conceptualization, R.K.; methodology, R.K. and M.A.I.; software, R.K.; validation, R.K.; formal analysis, R.K., K.H.L., and I.T.Y.; investigation, R.K. and M.A.I.; resources, R.K.; data curation, R.K. and K.H.M.; writing—original draft preparation, R.K.; writing—review and editing, R.K., M.A.I., K.H.L., and I.T.Y.; visualization, K.H.L. and I.T.Y.; supervision, R.K. and M.A.I. project administration, R.K. and M.A.I.; funding acquisition, M.A.I. All authors have read and agreed to the published version of the manuscript.

Funding: This research was funded by the National University of Sciences and Technology (NUST), Pakistan, Research Directorate recurring budget year 2021–22 under head Project Proposal with grant number “NUST-22-41-46”.

Data Availability Statement: All data used to support the findings of this study are included within the article.

Acknowledgments: This research was jointly conducted and supported by the School of Civil and Environmental Engineering (SCEE), Institute of Environmental Sciences and Engineering (IESE), National University of Sciences and Technology (NUST), Islamabad, Pakistan and Department of Chemical Engineering, Quaid-e-Awam University of Engineering, Science and Technology (QUEST), Nawabshah, Pakistan.

Conflicts of Interest: The authors declare no conflict of interest.

References

- Keller, A.A.; McFerran, S.; Lazareva, A.; Suh, S. Global life cycle releases of engineered nanomaterials. *J. Nanopart. Res.* **2013**, *15*, 1692. [[CrossRef](#)]
- Zhao, J.; Lin, M.; Wang, Z.; Cao, X.; Xing, B. Engineered nanomaterials in the environment: Are they safe? *Crit. Rev. Environ. Sci. Technol.* **2021**, *51*, 1443–1478. [[CrossRef](#)]
- Gottschalk, F.; Sun, T.; Nowack, B. Environmental concentrations of engineered nanomaterials: Review of modeling and analytical studies. *Environ. Pollut.* **2013**, *181*, 287–300. [[CrossRef](#)]
- Arvidsson, R. Risk Assessments Show Engineered Nanomaterials to Be of Low Environmental Concern. *Environ. Sci. Technol.* **2018**, *52*, 2436–2437. [[CrossRef](#)]
- Garner, K.L.; Suh, S.; Keller, A.A. Assessing the Risk of Engineered Nanomaterials in the Environment: Development and Application of the nanoFate Model. *Environ. Sci. Technol.* **2017**, *51*, 5541–5551. [[CrossRef](#)]
- Abbott Chalew, T.E.; Ajmani, G.S.; Huang, H.; Schwab, K.J. Evaluating nanoparticle breakthrough during drinking water treatment. *Environ. Health Perspect.* **2013**, *121*, 1161–1166. [[CrossRef](#)]

7. Pietroiusti, A.; Stockmann-Juvala, H.; Lucaroni, F.; Savolainen, K. Nanomaterial exposure, toxicity, and impact on human health. *Wiley Interdiscip. Rev. Nanomed. Nanobiotechnol.* **2018**, *10*, e1513. [[CrossRef](#)]
8. Fairbairn, E.A.; Keller, A.A.; Mädler, L.; Zhou, D.; Pokhrel, S.; Cherr, G.N. Metal oxide nanomaterials in seawater: Linking physicochemical characteristics with biological response in sea urchin development. *J. Hazard. Mater.* **2011**, *192*, 1565–1571. [[CrossRef](#)]
9. Cupi, D.; Hartmann, N.B.; Baun, A. Influence of pH and media composition on suspension stability of silver, zinc oxide, and titanium dioxide nanoparticles and immobilization of *Daphnia magna* under guideline testing conditions. *Ecotoxicol. Environ. Saf.* **2016**, *127*, 144–152. [[CrossRef](#)]
10. Popowich, A.; Zhang, Q.; Le, X.C. Removal of nanoparticles by coagulation. *J. Environ. Sci.* **2015**, *38*, 168–171. [[CrossRef](#)]
11. Rozman, U.; Klun, B.; Marolt, G.; Imperl, J.; Kalčíková, G. A study of the adsorption of titanium dioxide and zinc oxide nanoparticles on polyethylene microplastics and their desorption in aquatic media. *Sci. Total Environ.* **2023**, *888*, 164163. [[CrossRef](#)]
12. Khan, R.; Inam, M.A.; Akram, M.; Uddin, A.; Khan, S.; Yeom, I.T. Effect of Dissolved Organic Matter on Agglomeration and Removal of CuO Nanoparticles by Coagulation. *Processes* **2019**, *7*, 455. [[CrossRef](#)]
13. Wang, H.; Zhao, X.; Han, X.; Tang, Z.; Song, F.; Zhang, S.; Zhu, Y.; Guo, W.; He, Z.; Guo, Q. Colloidal stability of Fe₃O₄ magnetic nanoparticles differentially impacted by dissolved organic matter and cations in synthetic and naturally-occurred environmental waters. *Environ. Pollut.* **2018**, *241*, 912–921. [[CrossRef](#)] [[PubMed](#)]
14. Yadav, P.K.; Kochar, C.; Taneja, L.; Tripathy, S.S. Study on dissolution behavior of CuO nanoparticles in various synthetic media and natural aqueous medium. *J. Nanopart. Res.* **2022**, *24*, 122. [[CrossRef](#)]
15. Khan, R.; Inam, M.; Iqbal, M.; Shoaib, M.; Park, D.; Lee, K.; Shin, S.; Khan, S.; Yeom, I. Removal of ZnO Nanoparticles from Natural Waters by Coagulation-Flocculation Process: Influence of Surfactant Type on Aggregation, Dissolution and Colloidal Stability. *Sustainability* **2019**, *11*, 17. [[CrossRef](#)]
16. Gomez-Caballero, L.F.; Pichardo-Molina, J.L.; Briones, J.; Oyarzún, S.; Denardin, J.C.; Basurto-Islas, G. Facile synthesis of Fe₃O₄ nanoparticles at room temperature coated with meso-2, 3-dimercaptosuccinic acid for improved biocompatibility. *J. Nanopart. Res.* **2023**, *25*, 66. [[CrossRef](#)]
17. Crittenden, J.C.; Trussell, R.R.; Hand, D.W.; Howe, K.J.; Tchobanoglous, G. *MWH's Water Treatment: Principles and Design*; John Wiley & Sons: Hoboken, NJ, USA, 2012; ISBN 1118103777.
18. Wilhelm, C.; Billotey, C.; Roger, J.; Pons, J.N.; Bacri, J.-C.; Gazeau, F. Intracellular uptake of anionic superparamagnetic nanoparticles as a function of their surface coating. *Biomaterials* **2003**, *24*, 1001–1011. [[CrossRef](#)]
19. Reddy, L.H.; Arias, J.L.; Nicolas, J.; Couvreur, P. Magnetic nanoparticles: Design and characterization, toxicity and biocompatibility, pharmaceutical and biomedical applications. *Chem. Rev.* **2012**, *112*, 5818–5878. [[CrossRef](#)]
20. Arenas, L.R.; Le Coustumer, P.; Gentile, S.R.; Zimmermann, S.; Stoll, S. Removal efficiency and adsorption mechanisms of CeO₂ nanoparticles onto granular activated carbon used in drinking water treatment plants. *Sci. Total Environ.* **2023**, *856*, 159261. [[CrossRef](#)]
21. Sun, J.; Gao, B.; Zhao, S.; Li, R.; Yue, Q.; Wang, Y.; Liu, S. Simultaneous removal of nano-ZnO and Zn²⁺ based on transportation character of nano-ZnO by coagulation: Enteromorpha polysaccharide compound polyaluminum chloride. *Environ. Sci. Pollut. Res.* **2017**, *24*, 5179–5188. [[CrossRef](#)]
22. Keawchouy, S.; Na-Phatthalung, W.; Keaonaborn, D.; Jaichuedee, J.; Musikavong, C.; Sinyoung, S. Enhanced coagulation process for removing dissolved organic matter, microplastics, and silver nanoparticles. *J. Environ. Sci. Health Part A* **2022**, *57*, 1084–1098. [[CrossRef](#)] [[PubMed](#)]
23. Sousa, V.S.; Corniciuc, C.; Teixeira, M.R. The effect of TiO₂ nanoparticles removal on drinking water quality produced by conventional treatment C/F/S. *Water Res.* **2017**, *109*, 1–12. [[CrossRef](#)] [[PubMed](#)]
24. Maurizi, L.; Bisht, H.; Bouyer, F.; Millot, N. Easy route to functionalize iron oxide nanoparticles via long-term stable thiol groups. *Langmuir* **2009**, *25*, 8857–8859. [[CrossRef](#)]
25. Yip, N.Y.; Tiraferri, A.; Phillip, W.A.; Schiffman, J.D.; Hoover, L.A.; Kim, Y.C.; Elimelech, M. Thin-film composite pressure retarded osmosis membranes for sustainable power generation from salinity gradients. *Environ. Sci. Technol.* **2011**, *45*, 4360–4369. [[CrossRef](#)] [[PubMed](#)]
26. Bolster, C.H.; Mills, A.L.; Hornberger, G.M.; Herman, J.S. Spatial distribution of deposited bacteria following miscible displacement experiments in intact cores. *Water Resour. Res.* **1999**, *35*, 1797–1807. [[CrossRef](#)]
27. Stankus, D.P.; Lohse, S.E.; Hutchison, J.E.; Nason, J.A. Interactions between natural organic matter and gold nanoparticles stabilized with different organic capping agents. *Environ. Sci. Technol.* **2011**, *45*, 3238–3244. [[CrossRef](#)]
28. Chowdhury, I.; Cwiertny, D.M.; Walker, S.L. Combined factors influencing the aggregation and deposition of nano-TiO₂ in the presence of humic acid and bacteria. *Environ. Sci. Technol.* **2012**, *46*, 6968–6976. [[CrossRef](#)]
29. Khan, R.; Inam, M.; Zam, S.; Park, D.; Yeom, I. Assessment of Key Environmental Factors Influencing the Sedimentation and Aggregation Behavior of Zinc Oxide Nanoparticles in Aquatic Environment. *Water* **2018**, *10*, 660. [[CrossRef](#)]
30. Sevin, E.; Ertas, F.S.; Ulusoy, G.; Ozen, C.; Acar, H.Y. Meso-2,3-dimercaptosuccinic acid: From heavy metal chelation to CdS quantum dots. *J. Mater. Chem.* **2012**, *22*, 5137–5144. [[CrossRef](#)]
31. Cha, Y.J.; Kim, M.J.; Choa, Y.H.; Kim, J.; Nam, B.; Lee, J.; Kim, D.H.; Kim, K.H. Synthesis and characterizations of surface-coated superparamagnetic magnetite nanoparticles. *IEEE Trans. Magn.* **2010**, *46*, 443–446. [[CrossRef](#)]

32. Honda, R.J.; Keene, V.; Daniels, L.; Walker, S.L. Removal of TiO₂ Nanoparticles During Primary Water Treatment: Role of Coagulant Type, Dose, and Nanoparticle Concentration. *Environ. Eng. Sci.* **2014**, *31*, 127–134. [[CrossRef](#)] [[PubMed](#)]
33. Tang, H.; Xiao, F.; Wang, D. Speciation, stability, and coagulation mechanisms of hydroxyl aluminum clusters formed by PACl and alum: A critical review. *Adv. Colloid Interface Sci.* **2015**, *226*, 78–85. [[CrossRef](#)] [[PubMed](#)]
34. Baalousha, M.; Nur, Y.; Römer, I.; Tejamaya, M.; Lead, J.R. Effect of monovalent and divalent cations, anions and fulvic acid on aggregation of citrate-coated silver nanoparticles. *Sci. Total Environ.* **2013**, *454*, 119–131. [[CrossRef](#)] [[PubMed](#)]
35. Torkzaban, S.; Bradford, S.A.; Wan, J.; Tokunaga, T.; Masoudih, A. Release of quantum dot nanoparticles in porous media: Role of cation exchange and aging time. *Environ. Sci. Technol.* **2013**, *47*, 11528–11536. [[CrossRef](#)]
36. Zhang, Y.; Chen, Y.; Westerhoff, P.; Hristovski, K.; Crittenden, J.C. Stability of commercial metal oxide nanoparticles in water. *Water Res.* **2008**, *42*, 2204–2212. [[CrossRef](#)] [[PubMed](#)]
37. Chen, K.L.; Elimelech, M. Interaction of fullerene (C60) nanoparticles with humic acid and alginate coated silica surfaces: Measurements, mechanisms, and environmental implications. *Environ. Sci. Technol.* **2008**, *42*, 7607–7614. [[CrossRef](#)]

Disclaimer/Publisher’s Note: The statements, opinions and data contained in all publications are solely those of the individual author(s) and contributor(s) and not of MDPI and/or the editor(s). MDPI and/or the editor(s) disclaim responsibility for any injury to people or property resulting from any ideas, methods, instructions or products referred to in the content.